Clinical Radiology 79 (2024) e759–e766

Contents lists available at ScienceDirect

Clinical Radiology

journal homepage: www.clinicalradiologyonline.net

The hindbrain and cortico-reticular pathway in adolescent idiopathic scoliosis

R.C.C. Soh [a,b,†], B.Z. Chen [a,†], S. Hartono [b,c], M.S. Lee [a], W. Lee [a], S.L. Lim [a], J. Gan [d], B. Maréchal [e,f,g], L.L. Chan [a,b,*], Y.L. Lo [b,c]

[a] *Singapore General Hospital, Singapore*
[b] *Duke-NUS Medical School, Singapore*
[c] *National Neuroscience Institute, Singapore*
[d] *Siemens Healthineers, Singapore*
[e] *Advanced Clinical Imaging Technology, Siemens Healthcare AG, Lausanne, Switzerland*
[f] *Centre Hospitalier Universitaire Vaudois (CHUV), Lausanne, Switzerland*
[g] *Signal Processing Laboratory (LTS 5), École Polytechnique Fédérale de Lausanne (EPFL), Lausanne, Switzerland*

ARTICLE INFORMATION

Article history:
Received 15 February 2023
Received in revised form
9 January 2024
Accepted 18 January 2024

AIM: To characterise the corticoreticular pathway (CRP) in a case–control cohort of adolescent idiopathic scoliosis (AIS) patients using high-resolution slice-accelerated readout-segmented echo-planar diffusion tensor imaging (DTI) to enhance the discrimination of small brainstem nuclei in comparison to automated whole-brain volumetry and tractography and their clinical correlates.

MATERIALS AND METHODS: Thirty-four participants (16 AIS patients, 18 healthy controls) underwent clinical and orthopaedic assessments and brain magnetic resonance imaging (MRI) on a 3 T MRI machine. Automated whole-brain volume-based morphometry, tract-based spatial statistics analysis, and manual CRP tractography by two independent raters were performed. Intra-rater and inter-rater agreement of DTI metrics from CRP tractography were assessed by intraclass correlation coefficient. Normalised structural brain volumes and DTI metrics were compared between groups using Student's *t*-tests. Linear correlation analysis between imaging parameters and clinical scores was also performed.

RESULTS: AIS patients demonstrated a significantly larger pons volume compared to controls (p=0.006). Significant inter-side CRP differences in mean (p=0.02) and axial diffusivity (p=0.01) were found in patients only. Asymmetry in CRP fractional anisotropy significantly correlated with the Cobb angle (p=0.03).

CONCLUSION: Relative pontine hypertrophy and asymmetry in CRP DTI metrics suggest central supranuclear inter-hemispheric imbalance in AIS, and support the role of the CRP in

* Guarantor and correspondent: L.L. Chan, Singapore General Hospital, Outram Road, 169608, Singapore. Tel.: +65 6321 4229.
E-mail address: ling2chanSGH@gmail.com (L.L. Chan).
† These authors contributed equally to the study.

https://doi.org/10.1016/j.crad.2024.01.027

axial muscle tone. Longitudinal evaluation of CRP DTI metrics in the prediction of AIS progression may be clinically relevant.

Introduction

Adolescent idiopathic scoliosis (AIS) is a progressive musculoskeletal disease characterised by a lateral spinal deformity and a Cobb angle >10°.[1] It affects up to 7.5% of adolescents, with a female predilection.[1] AIS progression may lead to severe back pain requiring surgical intervention. Apart from spinal lateral curvature, vestibular, postural, and locomotor dysfunction have been observed in patients with AIS.[2,3] Neurophysiological evidence from transcranial magnetic stimulation and intraoperative monitoring of motor-evoked potentials and somatosensory evoked potentials point towards an inter-hemispheric imbalance of motor inhibition and output, possibly related to anomalous sensorimotor integration in AIS patients, as distinct from that in adult degenerative scoliosis. These support an underlying neurological aetiopathogenetic basis.[4,5]

The corticoreticular pathway (CRP), as part of the corticoreticulospinal tract, plays an important role in truncal muscular tone and posture, and locomotion.[6,7] Corticoreticular fibres are a major extrapyramidal output pathway from the premotor cortex to the brainstem that integrate with the reticulospinal neurons through widespread projections within the pontomedullary reticular formation[8]; however, the role of the CRP in AIS has not been explored.

Recent fully automated tools for brain morphometry have allowed objective evaluation of regional volumetric changes in neurological disorders.[9,10] Tract-Based Spatial Statistics (TBSS) is also an objective, whole-brain, open-source tool for analysis of diffusion tensor imaging (DTI) data,[11] based on anisotropic water molecular movement in white matter.[12] Through diffusion tensor data gathered across voxels, mathematical models of fibre tracts reconstructions that simulate anatomical connectivity extrapolate information about the state of neural tissue micro-architecture; however, tractography of specific white matter tracts of interest that traverse the brainstem, such as the CRP, is not included in the TBSS suite of tools.

Tractography of the CRP requires careful discrimination of the small brainstem nuclei, which is challenging with the distortion prevalent in the posterior fossa on the often employed single-shot echo-planar DTI sequences. Multi-shot or readout-segmented diffusion-weighted echo-planar imaging, such as RESOLVE-DTI,[13,14] partitions frequency encoding of the k-space into shorter segments and affords superior image quality with the shorter echo spacing and train length. The resultant longer scan time is mitigated by coupling with slice acceleration, with no significant net scan time penalty. In this study, slice-accelerated RESOLVE-DTI was incorporated into a case–control, multimodal quantitative magnetic resonance imaging (MRI) approach to characterise changes in the CRP in AIS, in comparison to automated whole-brain volumetry and tractography, and their clinical correlates. It was hypothesised that AIS patients would demonstrate structural hindbrain and diffusion changes in the CRP, which would correlate with the Cobb angle.

Materials and methods

This study was approved by the local Centralised Institutional Review Board. Informed consent was obtained from all participating subjects or parents of subjects <21 years old.

Clinical

Thirty-four subjects comprising 18 controls and 16 neurologically intact patients diagnosed with AIS based on a national screening programme were included. The patients were reviewed at the adolescent spinal deformity clinic in a tertiary referral hospital before recruitment. Exclusion criteria included contraindications to MRI, concomitant neurological/spinal disorders, and spinal/head injury. Healthy volunteers of similar age and gender to the AIS patients, screened by the clinical team to exclude scoliosis, were recruited into the study. Handedness was assessed using the Edinburgh Handedness Inventory Scale. The clinical demographics of the subjects are detailed in Table 1. The cohorts were dominantly female. Full orthopaedic assessment including the Lenke classification for AIS, site, and side of primary curve, Cobb angle, and number of spinal segments involved in the scoliosis was made for all AIS patients and detailed in Table 2.

Brain imaging

All participants underwent MRI brain on a 3 T MRI machine (MAGNETOM Skyra, Siemens Healthcare, Erlangen, Germany) using a 32-channel head coil. The parameters of the sequences employed were (1) T1-weighted sagittal 3D magnetisation-prepared rapid gradient echo (MPRAGE) acquisition: 2,300 ms repetition time (TR), 2.88 ms echo time (TE), 900 ms inversion time (TI), 256 × 256 matrix, 1 × 1 × 1 mm^3 resolution, GeneRalised Autocalibrating Partially Parallel Acquisition (GRAPPA) factor of 2; and (2) simultaneous multi-slice (SMS) RESOLVE-DTI[11,12]: 3,000 ms TR, 70 ms TE, RESOLVE factor of = 5, SMS factor of = 3, GRAPPA factor of = 2, 64 non-collinear diffusion-sensitising gradient directions with b-value of = 0, 1,000 s/mm^2, 128 × 128 matrix,

Table 1
Study demographics and clinical characteristics.

Groups	Adolescent idiopathic scoliosis patients	Controls	*p*-Value
No.	16	18	–
Age (years)	21.2 ± 2.3 (17–27)	21.3 ± 2.2 (16–25)	0.92
Gender (M/F)	6/10	4/14	0.33
Handedness (right/mixed)	14/2	16/2	0.90
Side of major curvature	12 right thoracic/4 left thoraco-lumbar or lumbar	–	–
Cobb angle (degrees)	47 ± 13.5 (29–78)	–	–
No. of vertebral levels	9 ± 3.3 (4–15)	–	–

Values shown for age, Cobb angle, and number of vertebral levels are mean ± SD (range). Demographic and clinical characteristics variables were compared by their mean or proportions between adolescent idiopathic scoliosis patients and healthy controls using Student's *t*-test or Mann–Whitney *U*-test, respectively.

$2 \times 2 \times 2.5$ mm^3 resolution, in 60 contiguous sections parallel to the anterior commissure–posterior commissure line.

Image analysis

Automated brain volume-based morphometry was performed on MPRAGE images using the Morphobox prototype[6] to estimate individual brain structure volumes in millilitres, which were normalised as a percentage of total intracranial volume. Voxel-wise statistical analysis of fractional anisotropy (FA) from the DTI data was carried out using Tract-Based Spatial Statistics (TBSS) in the FMRIB Software Library (www.fmrib.ox.ac.uk/fsl/).[11] Image normalisation was performed by registering the individual DTI images to the FMRIB58 standard-space image as the target in FSL for TBSS analysis. TBSS projected all subject FA data onto an averaged FA tract skeleton, before applying voxel-wise cross-subject statistics. The Johns Hopkins University white matter tractography atlas, based on the DTI database of the International Consortium of Brain Mapping (ICBM), was used to extract the DTI parameters from white matter tracts.

Following previously described methodology for identification of the CRP, tractography of the CRP was performed on the individual DTI space by an experienced MRI technologist using a deterministic tracking algorithm in DSI studio (Fiber Tractography Lab, University of Pittsburgh, Pennsylvania, USA; Fig 1) under the supervision of a neuroradiologist with more than two decades of experience. A seed region of interest (ROI) was placed at the reticular formation of the medulla. First and second target ROIs were placed at the midbrain tegmentum and premotor cortex, respectively. The ROI sizes employed were fixed and defined. Fibre tracking was performed using standardised FA threshold of >0.2 and angle threshold of $<70^\circ$. The CRP streamlines were inspected visually to verify their expected anatomical course through the ipsilateral subcortical white matter and brainstem, with erroneous streamlines or crossing fibres deleted. Quantitative DTI parameters were extracted, namely FA, mean (MD), radial (RD), and axial diffusivity (AD) of the CRP streamlines. The procedure was repeated by the same technologist 1-week later and independently by a second experienced MRI technologist for intra-rater and inter-rater reliability analysis, respectively. Quantitative DTI parameters were additionally extracted from the pons using DSI studio.

Table 2
Clinical orthopaedic parameters in adolescent idiopathic scoliosis patients.

No.	Lenke	Primary site	Cobb angle (degrees)	No. of vertebral levels	Structural curves
1	3	Right	52	12	T5-L4
2	1	Right	55	8	T5-T12
3	1	Right	63	7	T6-T12
4	3	Right	78	12	T5-L4
5	1	Right	53	9	T5-L1
6	4	Left	43	15	T2-L4
7	1	Right	33	4	T5-T8
8	1	Right	45	8	T8-L3
9	5	Left	25	6	T10-L3
10	1	Right	45	8	T5-T12
11	2	Left	50	13	T2-L2
12	4	Left	45	15	T2-L4
13	3	Right	58	12	T5-L4
14	5	Right	29	6	T10-L3
15	1	Right	46	8	T4-T11
16	1	Right	32	8	T4-T11

Statistical analysis

Statistical analysis was conducted using the Statistical Package for Social Science software. Intra- and inter-rater reliability of CRP tractography were assessed by intraclass correlation coefficient and Dice coefficient analysis. Student's *t*-tests were carried out to compare the structural brain volume data and DTI parameters from whole-brain TBSS analysis and CRP tractography between AIS patients and controls. Linear correlation analysis was performed to evaluate the association between imaging parameters with clinical scores. Statistical significance was defined at $p<0.05$.

Results

Twelve (75%) patients had a right-sided primary curve. In 14 (87.5%) patients, the primary curve was thoracic (Lenke 1–4) based on the Lenke classification. There was no evidence of Arnold Chiari malformation or syringohydromyelia at the craniocervical junction and included upper cervical cord on the structural T1 series in all subjects.

The normalised pons volume was larger in AIS patients (1.42 ± 0.12%; absolute volume: 15.94 ± 1.47 cm^3) compared to controls (1.31 ± 0.10%; absolute volume: 15.07 ± 1.93 cm^3; $p=0.006$), and the left insula smaller in

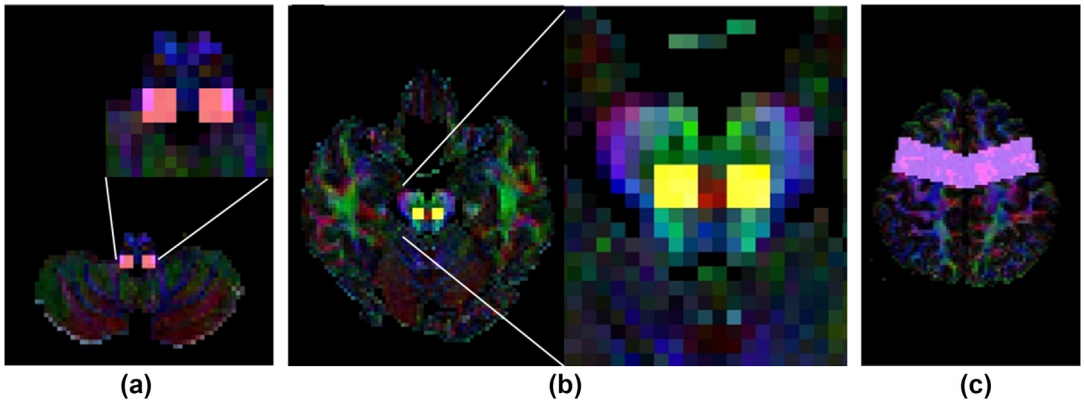

Figure 1 ROI placement for CRP tractography. Axial colour FA images demonstrating placement of (a) a seed ROI at the reticular formation of the medulla with magnified view (inset), (b) first target ROI at the midbrain tegmentum with magnified view (right), and (c) second target ROI at the premotor cortex.

AIS patients (0.55 ± 0.04%; absolute volume: 6.21 ± 0.71 cm^3) compared to controls (0.57 ± 0.02%; absolute volume: 6.61 ± 0.54 cm^3; p=0.04). DTI parameters extracted from the pons showed no significant difference in FA (p=0.17) and MD (p=0.24) between the groups: AIS patients (FA: 0.46 ± 0.02, MD: 0.91 ± 0.03) and controls (FA: 0.45 ± 0.02, MD: 0.92 ± 0.03).

In whole-brain TBSS voxel-wise analysis, there was a trend towards lower FA in the AIS group, albeit not statistically significant (AIS: 0.42 ± 0.02, HC: 0.43 ± 0.01; p=0.08). Further subsegmental analysis of the corpus callosum also showed no significant difference between the two groups (Electronic Supplementary Material Table S1).

A sample image of the CRP vis-à-vis corticospinal tract is depicted in Fig 2. Intra-rater and inter-rater Dice coefficients for the CRP streamlines were 0.88 (very good) and 0.73 (good), respectively. Both intra-rater and inter-rater intraclass correlation coefficients for all DTI parameters of the CRP streamlines were >0.9 (excellent). DTI parameters of the CRP were similar between patients and controls (Table 3); however, significant differences in MD (p=0.02) and AD (p=0.01) were observed between the left and right CRP streamlines in AIS patients, with higher MD and AD in the right CRP. Similar results were found after excluding two AIS patients who were ambidextrous (Electronic Supplementary Material Table S2). There was no asymmetry in DTI parameters between sides in the CRP streamlines in the control cohort (Table 4).

Left-right FA ratio of the CRP streamlines was found to have a statistically significant correlation with the magnitude of Cobb angle (p=0.03), with greater inter-side FA asymmetry associated with greater Cobb angle. There was no statistically significant correlation between tractography parameters and the total affected scoliosis segments (p=0.10); however, a statistically significant correlation between the normalised total ventricular volume (including lateral, third, and fourth ventricles) and the total number of vertebral levels affected by scoliosis (p=0.02) was noted. This was not significant for the Cobb angle (p=0.97; Table 5).

Discussion

The AIS patients had a larger pons than the controls on automated brain morphometry. Liu *et al.* also reported a significantly larger brainstem in AIS patients than controls.[2] Posture, proprioception, and equilibrium control functions are integrated by structures in and around the brainstem.[3,15,16] A hindbrain abnormality, and specifically one affecting the paramedian pontine reticular formation, linking motor, preocular motor nuclei and vestibular nuclei, has been implicated in AIS.[1,2,17] Preclinical studies have also shown that creating lesions in the pons and periaqueductal grey matter could induce scoliosis.[18] Hence, the present findings support the role of the hindbrain in the aetiopathogenesis of AIS.

The use of slice-accelerated RESOLVE-DTI in the present imaging protocol allowed for sampling of the k-space trajectory along the readout direction in separate partitioned segments, thereby reducing susceptibility artefacts and image blurring whilst reducing scan time.[13,14,19] This provided superior high-resolution depiction of the small brainstem nuclei that enabled excellent reproducibility of manual CRP tractography (Figs 1 and 2), as the latter required careful seed placement in hindbrain structures within the posterior fossa.[7,20] In spite of the increasing availability of various automated tract-based tractography software packages,[11,21] automated tract-based analysis of neural tracts of interest involving seed points in the brainstem remain elusive, partly related to the aforementioned reasons. The neuroanatomical location of the CRP streamlines in the present study was established in relation to the clinically robust tractography of the corticospinal tract, and familiarity with less clinically routine tractography of the spinothalamic tract and medial lemniscus.[22,23] The FA and MD values of the CRP in controls are also congruent with those reported in the literature.[7]

The CRP plays a critical role in motor function, being primarily responsible for innervation of the axial and proximal muscles, which are required for gross motor skills such as postural and gait control. DTI studies demonstrating

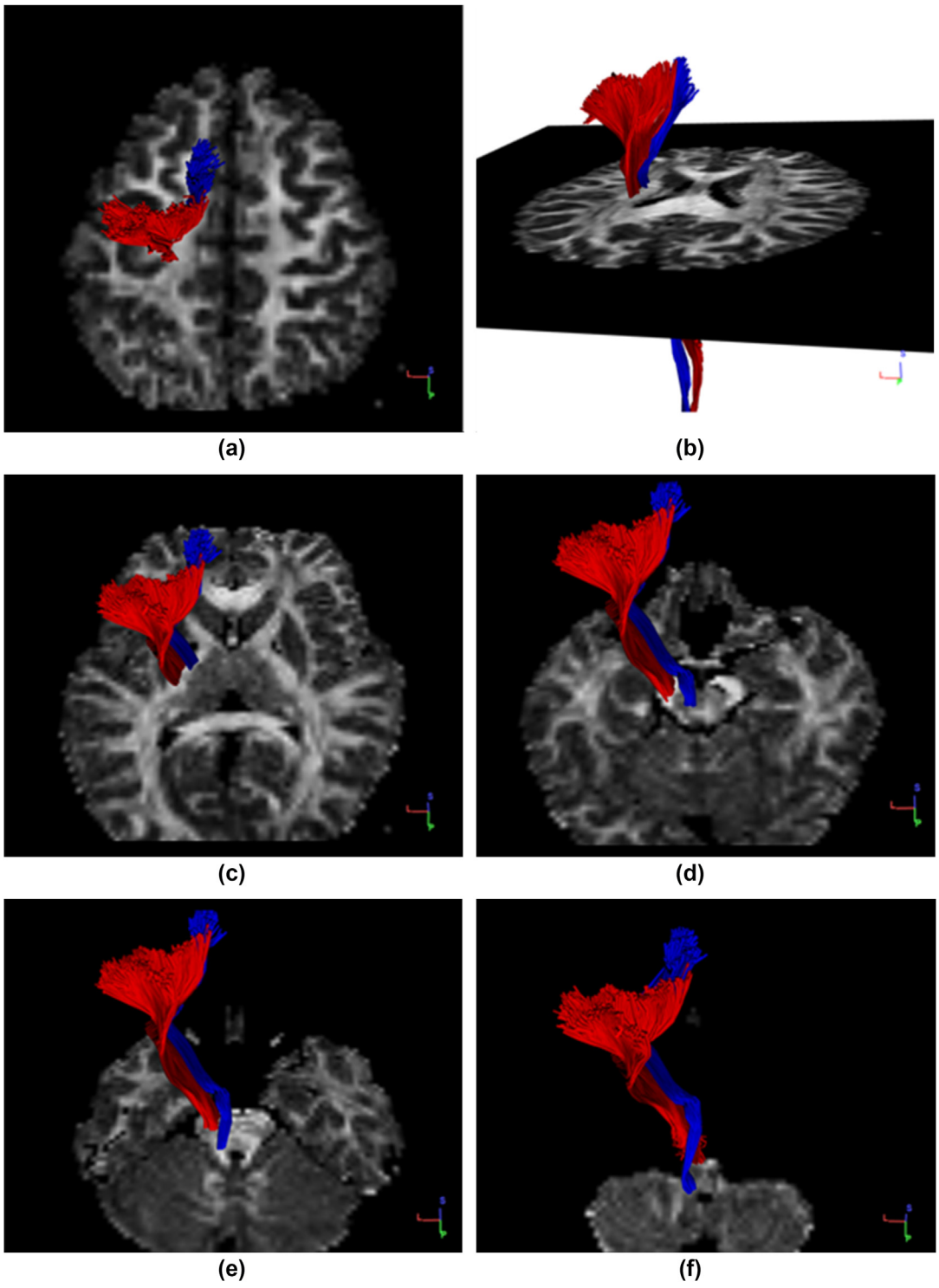

Figure 2 Three-dimensional depiction of the CRP streamlines in relation to the corticospinal tract (CST) projected on two-dimensional axial FA maps of DTI data. The CRP is validated with reference to the CST along its entire pathway as it descends from (a) the premotor cortex, (b) through the corona radiata, (c) posterior limb of the internal capsule anterior to the CST, (d) mesencephalic tegmentum in a medio-posterior direction, and traversing (e) the pontine reticular formation, before terminating at (f) the pontomedullary reticular formation. (CRP: blue and CST: red).

loss of integrity of the CRP have been reported in sarcopenia, stroke, and post-traumatic brain injury.[20,24] Significant inter-side differences were found in the DTI parameters of the CRP only in the AIS patients. Similar trends of higher MD and AD in the right CRP (Table 4) remain when only right-handed patients were analysed (Electronic Supplementary Material Table S2), suggesting that these are probably not related to patient handedness. Microstructural tissue alterations causing a rise in MD and AD are generally accompanied by a drop in FA, according to the FA equation;

Table 3
Comparison of DTI parameters from CRP tractography between AIS patients and healthy controls.

Structure	DTI parameter	AIS	Controls	*p*-Value
CRP (right)	FA	0.49 ± 0.03	0.49 ± 0.02	0.57
	MD	0.84 ± 0.05	0.83 ± 0.02	0.78
	AD	1.34 ± 0.08	1.33 ± 0.03	0.53
	RD	0.58 ± 0.05	0.58 ± 0.03	0.97
CRP (left)	FA	0.49 ± 0.02	0.49 ± 0.02	0.63
	MD	0.82 ± 0.04	0.84 ± 0.03	0.08
	AD	1.31 ± 0.06	1.34 ± 0.05	0.09
	RD	0.57 ± 0.04	0.59 ± 0.03	0.14

Values shown are mean ± SD; and MD, AD and R values are $x10^{-3}$ mm^2/s.
AIS, adolescent idiopathic scoliosis; AD, axial diffusivity; CRP, corticoreticular pathway; DTI, diffusion tensor imaging; FA, fractional anisotropy; MD, mean diffusivity; RD, radial diffusivity.

Table 5
Correlation between imaging parameters and clinical orthopaedic assessment.

Clinical correlation	Cobb angle		No. of vertebral levels	
	R	*p*-Value	R	*p*-Value
No. of vertebral levels	0.43	0.10	–	–
FA left:right ratio	0.61	0.03[a]	0.08	0.78
Total ventricular volume (ml)	−0.01	0.97	0.56	0.02[a]

Linear correlation analysis was performed to evaluate the association between imaging parameters with clinical scores. FA left:right ratio is defined as the ratio between the FA on the left to the right CRP tract. Total ventricular volume (left and right lateral, third and fourth ventricles) as derived from automated brain morphometry.
FA, fractional anisotropy.
[a] $p < 0.05$.

however, the present results also showed a rise in RD (albeit insignificant), which could explain the unchanged FA (i.e., a negligibly reduced) value. The DTI changes may be related to different *in vivo* microstructural processes (which may co-exist), such as axonal damage, changes to myelination, membrane permeability, fibre density, axonal diameter and/or congruence in orientation. Preclinical studies in AIS using advanced diffusion modelling approaches at higher field strengths would be needed to characterise these properly.[25,26] The typical "S" shape of the spinal scoliosis (with either a primary right-sided thoracic or left-sided lumbar/thoracolumbar curve) as is prevalent in the normal population of AIS patients[27–29] gives relevance to the DTI findings. A statistically significant correlation between inter-side FA asymmetry and the Cobb angle was found. These findings corroborate with proposals of the central nervous system being the aetiopathogenetic site in AIS.[1,8] They bring new evidence for supranuclear white matter microstructural alterations, albeit whether these DTI changes in the CRP signify primary versus secondary compensatory responses to brainstem developmental abnormality are moot. Besides highlighting the important role of the CRP in axial muscular tone, the present findings suggest a plausible role for longitudinal evaluation of the CRP using DTI in the prediction of AIS progression.

Table 4
Comparison of DTI parameters between left and right CRP in AIS patients and healthy controls.

Structure	DTI parameter	CRP (left)	CRP (right)	*p*-Value
AIS patients	FA	0.49 ± 0.02	0.49 ± 0.03	0.71
	MD	0.82 ± 0.04	0.84 ± 0.05	0.02[a]
	AD	1.31 ± 0.06	1.34 ± 0.08	0.01[a]
	RD	0.57 ± 0.04	0.58 ± 0.05	0.09
Controls	FA	0.49 ± 0.02	0.49 ± 0.02	0.98
	MD	0.84 ± 0.03	0.83 ± 0.02	0.30
	AD	1.34 ± 0.05	1.33 ± 0.03	0.26
	RD	0.59 ± 0.03	0.58 ± 0.03	0.53

Values shown are mean ± SD; and MD, AD and R values are × 10^{-3} mm^2/s.
AIS, adolescent idiopathic scoliosis; AD, axial diffusivity; CRP, corticoreticular pathway; DTI, diffusion tensor imaging; FA, fractional anisotropy; MD, mean diffusivity; RD, radial diffusivity.
[a] $p < 0.05$.

The present findings of inter-hemispheric differences concur with findings of inter-side imbalance from studies employing functional MRI utilising blood oxygenation level-dependent contrast and neurophysiological assessments in AIS patients.[4,5,30,31] Intraoperative studies using electrical stimulation found larger amplitudes in ipsilateral motor-evoked potentials of scoliosis patients, suggesting possible contribution of uncrossed descending pathways, of which the CRP may be involved.[4,32,33] Inter-side differences in abnormal somatosensory evoked potentials were also found in patients with AIS compared to congenital scoliosis by Chen *et al.*[31] Asymmetry of cortical excitability elicited with transcranial magnetic stimulation[5] and increased asymmetry in cortical activation after motor activation demonstrated using functional MRI[30] have also been reported. The present findings provide anatomical DTI quantitative data corroborating with this evidence of functional neurological asymmetry.

Although the difference in normalised total ventricular volume was not statistically significant between groups, there was a positive correlation between normalised total ventricular volume and the total number of vertebral levels affected by scoliosis (p=0.02) in the AIS patients. Co-existing neuraxial abnormalities are known to exist in AIS patients, which could impact surgical risks and outcomes, including risks of neurological injury and curve progression following standard posterior arthrodesis.[34] A meta-analysis by Faloon *et al.* showed the most common neuraxial abnormalities to be syringomyelia (35%), Arnold–Chiari Type 1 malformation with syrinx (28%), and isolated Arnold–Chiari Type 1 malformation (25%).[35] To date, there is lack of consensus on MRI screening guidelines, with variations existing across different centres. Recommended indications for MRI in the literature include male gender, early onset (<11 years old), pain, atypical curve patterns (left-sided thoracic deformity, short segmental involvement [four to six levels], decreased vertebral rotation, absence of thoracic apical segment lordosis, hyperkyphosis, double thoracic curvatures), rapid progression, and abnormal neurological findings on physical examination.[34–36] Spinal MRI screening was not performed in the AIS patients given the lack of atypical clinical features on orthopaedic

assessment. Nevertheless, none of the present AIS patients had abnormal neurological examinations or findings of an Arnold–Chiari malformation or syringohydromyelia on brain MRI, suggesting an intraspinal anomaly to be unlikely. Given that the systolic pulse wave is well established as the primary impetus for CSF propulsion and circulation in the subarachnoid space, it is postulated that findings of a larger total ventricular volume correlating with an overall longer total vertebral segment of scoliosis involvement may be explained by greater impedance to CSF flow in view of a more sinuous CSF path within the central canal of the spinal cord in the present AIS patients.[37]

TBSS provided automated, objective whole-brain DTI analysis without time-consuming ROI prescriptions. The present AIS patients had overall lower FA in the white matter skeleton than healthy controls, but the difference was not statistically significant (p=0.077). Similarly, Xue *et al.* found no significant difference in FA between AIS and HC using whole-brain TBSS analysis.[38] The corpus callosum, the major white matter structure affording inter-hemispheric connectivity and inter-side coordination, has been of great interest to researchers in AIS[38–40]; however, conflicting results for DTI analysis of the corpus callosum exist in the literature. Xue *et al.* found significant FA differences only in the genu and splenium, while Joly *et al.* observed differences only in the body of the corpus callosum in AIS patients compared to controls.[38,40] The present study found no significant differences in FA between groups in the subsegmental regional DTI analysis of the corpus callosum (Electronic Supplementary Material Table S1). TBSS may be sensitive to registration errors and differences in templates used for corpus callosum segmentation, segmentation approaches (manual versus automated versus mixed) and sample sizes could also contribute to the conflicting results across studies.

Although the aetiopathogenesis of AIS remains poorly understood, multifactorial contributions from genetic polymorphisms, environmental triggers, disrupted hormonal and metabolic signalling, neuro-osseous disharmony, and biomechanical elements have been proposed.[1] This study in AIS showed that structural and diffusion MRI are sensitive non-invasive tools with potential for tracking and monitoring of disease progression in relation to clinical markers. The pontine volumetric and diffusion-based CRP changes, in association with the Cobb angle, add further to the body of evidence that the hindbrain plays a central role in AIS. More advanced diffusion modelling and analytics, in conjunction with electrophysiological data, would better dissect the complex connectomics of the CRP for axial postural control, and shed further light on the associated underlying microstructural changes.

The major limitation of the present study lies in the small sample size; however, the cohort numbers are similar to many AIS studies in the literature. Besides, the majority of the present patients were Lenke 1 and 3, which correlates well with a previous large radiographic study documenting the prevalence of curve patterns in AIS.[41] The distribution of females to males in the present study cohort also mirrors the prevalence of AIS.[27,28] Hence, the finding of hindbrain differences between healthy controls and AIS patients in the present exploratory study are therefore a fair representation of the majority of AIS patients. Future work on CRP tractography in a larger adolescent cohort, including the effects of the sex hormones, would be interesting. Higher-order diffusion techniques such as diffusion kurtosis imaging or diffusion spectrum imaging could also be explored to elucidate the non-Gaussian diffusion or crossing fibres in the CRP.

In conclusion, AIS patients showed pontine hypertrophy and asymmetry of diffusion parameters in the CRP, with the latter showing significant correlation with the Cobb angle. These findings highlight the importance of the brainstem in the integration of truncal muscle tone, and the potential role of longitudinal DTI evaluation of the CRP in the tracking of AIS progression.

Conflict of interest

The authors declare the following financial interests/personal relationships which may be considered as potential competing interests: Benedicte Marechal reports a relationship with Siemens Healthcare AG that includes: employment. Julian Gan reports a relationship with Siemens Healthineers that includes: employment. If there are other authors, they declare that they have no known competing financial interests or personal relationships that could have appeared to influence the work reported in this paper.

Acknowledgements

The authors are grateful for the support from the staff of the Department of Neurology, Singapore General Hospital, and the National Neuroscience Institute, and the excellent team of radiographers and clinical research coordinators at the Department of Diagnostic Radiology, Singapore General Hospital. Funding for the study was obtained from the SingHealth Foundation, SGH Integrated Fund GZSHF9005401.

Appendix A. Supplementary data

Supplementary data to this article can be found online at https://doi.org/10.1016/j.crad.2024.01.027.

References

1. Cheng JC, Castelein RM, Chu WC, *et al.* Adolescent idiopathic scoliosis. *Nat Rev Dis Primers* 2015;**1**:15030, https://doi.org/10.1038/nrdp.2015.30.
2. Liu T, Chu WC, Young G, *et al.* MR analysis of regional brain volume in adolescent idiopathic scoliosis: neurological manifestation of a systemic disease. *J Magn Reson Imaging* 2008;**27**(4):732–6. https://doi.org/10.1002/jmri.21321.
3. Lowe TG, Edgar M, Margulies JY, *et al.* Etiology of idiopathic scoliosis: current trends in research. *J Bone Jt Surg Am* 2000;**82**(8):1157–68. https://doi.org/10.2106/00004623-200008000-00014.
4. Lo YL, Teo A, Tan YE, *et al.* Motor and somatosensory abnormalities are significant etiological factors for adolescent idiopathic scoliosis. *J Neurol Sci* 2015;**359**(1–2):117–23. https://doi.org/10.1016/j.jns.2015.10.048.

5. Doménech J, Tormos JM, Barrios C, *et al*. Motor cortical hyperexcitability in idiopathic scoliosis: could focal dystonia be a subclinical etiological factor? *Eur Spine J* 2010;**19**(2):223–30. https://doi.org/10.1007/s00586-009-1243-y.
6. Jang SH, Lee SJ. Corticoreticular tract in the human brain: a mini review. *Front Neurol* 2019;**10**:1188. https://doi.org/10.3389/fneur.2019.01188.
7. Yeo SS, Chang MC, Kwon YH, *et al*. Corticoreticular pathway in the human brain: diffusion tensor tractography study. *Neurosci Lett* 2012;**508**(1):9–12. https://doi.org/10.1016/j.neulet.2011.11.030.
8. Matsuyama K, Mori F, Nakajima K, *et al*. Locomotor role of the corticoreticular–reticulospinal–spinal interneuronal system. *Prog Brain Res* 2004;**143**:239–49. https://doi.org/10.1016/S0079-6123(03)43024-0.
9. Schmitter D, Roche A, Maréchal B, *et al*. Alzheimer's Disease Neuroimaging Initiative. An evaluation of volume-based morphometry for prediction of mild cognitive impairment and Alzheimer's disease. *Neuroimage Clin* 2014;**7**:7–17. https://doi.org/10.1016/j.nicl.2014.11.001.
10. Fang E, Fartaria MJ, Ann CN, *et al*. Clinical correlates of white matter lesions in Parkinson's disease using automated multi-modal segmentation measures. *J Neurol Sci* 2021;**427**:117518, https://doi.org/10.1016/j.jns.2021.117518.
11. Smith SM, Jenkinson M, Johansen-Berg H, *et al*. Tract-based spatial statistics: voxelwise analysis of multi-subject diffusion data. *Neuroimage* 2006;**31**(4):1487–505. https://doi.org/10.1016/j.neuroimage.2006.02.024.
12. Alexander AL, Lee JE, Lazar M, *et al*. Diffusion tensor imaging of the brain. *Neurotherapeutics* 2007;**4**(3):316–29. https://doi.org/10.1016/j.nurt.2007.05.011.
13. Koh YH, Shih YC, Lim SL, *et al*. Evaluation of trigeminal nerve tractography using two-fold-accelerated simultaneous multi-slice readout-segmented echo planar diffusion tensor imaging. *Eur Radiol* 2021;**31**(2):640–9. https://doi.org/10.1007/s00330-020-07193-x.
14. Frost R, Jezzard P, Douaud G, *et al*. Scan time reduction for readout-segmented EPI using simultaneous multislice acceleration: diffusion-weighted imaging at 3 and 7 Tesla. Version 2. *Magn Reson Med* 2015;**74**(1):136–49. https://doi.org/10.1002/mrm.25391.
15. Simoneau M, Lamothe V, Hutin E, *et al*. Evidence for cognitive vestibular integration impairment in idiopathic scoliosis patients. *BMC Neurosci* 2009;**10**:102. https://doi.org/10.1186/1471-2202-10-102.
16. Lao ML, Chow DH, Guo X, *et al*. Impaired dynamic balance control in adolescents with idiopathic scoliosis and abnormal somatosensory evoked potentials. *J Pediatr Orthop* 2008;**28**(8):846–9. https://doi.org/10.1097/BPO.0b013e31818e1bc9.
17. Kong Y, Shi L, Hui SC, *et al*. Variation in anisotropy and diffusivity along the medulla oblongata and the whole spinal cord in adolescent idiopathic scoliosis: a pilot study using diffusion tensor imaging. *AJNR Am J Neuroradiol* 2014;**35**(8):1621–7. https://doi.org/10.3174/ajnr.A3912.
18. Barrios C, Arrotegui JI. Experimental kyphoscoliosis induced in rats by selective brain stem damage. *Int Orthop* 1992;**16**(2):146–51. https://doi.org/10.1007/BF00180206.
19. Rumpel H, Chong Y, Porter DA, *et al*. Benign versus metastatic vertebral compression fractures: combined diffusion-weighted MRI and MR spectroscopy aids differentiation. *Eur Radiol* 2013;**23**(2):541–50. https://doi.org/10.1007/s00330-012-2620-1.
20. Jang SH, Chang CH, Lee J, *et al*. Functional role of the corticoreticular pathway in chronic stroke patients. *Stroke* 2013;**44**(4):1099–104. https://doi.org/10.1161/STROKEAHA.111.000269.
21. Chen YJ, Lo YC, Hsu YC, *et al*. Automatic whole brain tract-based analysis using predefined tracts in a diffusion spectrum imaging template and an accurate registration strategy. *Hum Brain Mapp* 2015;**36**(9):3441–58. https://doi.org/10.1002/hbm.22854.
22. Kamali A, Kramer LA, Butler IJ, *et al*. Diffusion tensor tractography of the somatosensory system in the human brainstem: initial findings using high isotropic spatial resolution at 3.0 T. *Eur Radiol* 2009;**19**(6):1480–8. https://doi.org/10.1007/s00330-009-1305-x.
23. Lee W, Hartono S, Lo YL, *et al*. Identification of the somatosensory system using diffusion tensor tractography. In: *Proceedings of the European Society for magnetic resonance in medicine and biology (ESMRMB) 2019 congress*; 2019. p. 3–5 [Rotterdam, Netherlands].
24. Kwak SY, Kwak SG, Yoon TS, *et al*. Deterioration of brain neural tracts in elderly women with sarcopenia. *Am J Geriatr Psychiatry* 2019;**27**(8):774–82. https://doi.org/10.1016/j.jagp.2019.02.018.
25. Beaulieu C. The basis of anisotropic water diffusion in the nervous system—a technical review. *NMR Biomed* 2002;**15**:435–55. https://doi.org/10.1002/nbm.782.
26. Jones DK, Knösche TR, Turner R. White matter integrity, fiber count, and other fallacies: the do's and don'ts of diffusion MRI. *Neuroimage* 2013;**73**:239–54. https://doi.org/10.1016/j.neuroimage.2012.06.081.
27. Wong HK, Hui JH, Rajan U, *et al*. Idiopathic scoliosis in Singapore schoolchildren: a prevalence study 15 years into the screening program. *Spine (Phila Pa 1976)* 2005;**30**(10):1188–96. https://doi.org/10.1097/01.brs.0000162280.95076.bb.
28. Soucacos PN, Soucacos PK, Zacharis KC, *et al*. School-screening for scoliosis. A prospective epidemiological study in northwestern and central Greece. *J Bone Jt Surg Am* 1997;**79**(10):1498–503. https://doi.org/10.2106/00004623-199710000-00006.
29. Schlösser TPC, Semple T, Carr SB, *et al*. Scoliosis convexity and organ anatomy are related. *Eur Spine J* 2017;**26**(6):1595–9. https://doi.org/10.1007/s00586-017-4970-5.
30. Domenech J, García-Martí G, Martí-Bonmatí L, *et al*. Abnormal activation of the motor cortical network in idiopathic scoliosis demonstrated by functional MRI. *Eur Spine J* 2011;**20**(7):1069–78. https://doi.org/10.1007/s00586-011-1776-8.
31. Chen Z, Qiu Y, Ma W, *et al*. Comparison of somatosensory evoked potentials between adolescent idiopathic scoliosis and congenital scoliosis without neural axis abnormalities. *Spine J* 2014;**14**(7):1095–8. https://doi.org/10.1016/j.spinee.2013.07.465.
32. Lo YL, Dan YF, Tan YE, *et al*. Intraoperative monitoring study of ipsilateral motor evoked potentials in scoliosis surgery. Version 2. *Eur Spine J* 2006;**15**(Suppl 5):656–60. https://doi.org/10.1007/s00586-006-0190-0.
33. Lo YL, Dan YF, Teo A, *et al*. The value of bilateral ipsilateral and contralateral motor evoked potential monitoring in scoliosis surgery. *Eur Spine J* 2008;**17**(Suppl. 2):S236–8. https://doi.org/10.1007/s00586-007-0498-4.
34. Davids JR, Chamberlin E, Blackhurst DW. Indications for magnetic resonance imaging in presumed adolescent idiopathic scoliosis. *J Bone Jt Surg Am* 2004;**86**(10):2187–95. https://doi.org/10.2106/00004623-200410000-00009.
35. Faloon M, Sahai N, Pierce TP, *et al*. Incidence of neuraxial abnormalities is approximately 8% among patients with adolescent idiopathic scoliosis: a meta-analysis. *Clin Orthop Relat Res* 2018;**476**(7):1506–13. https://doi.org/10.1007/s11999.0000000000000196.
36. Diab M, Landman Z, Lubicky J, *et al*. Use and outcome of MRI in the surgical treatment of adolescent idiopathic scoliosis. *Spine (Phila Pa 1976)* 2011;**36**(8):667–71. https://doi.org/10.1097/BRS.0b013e3181da218c.
37. Whedon JM, Glassey D. Cerebrospinal fluid stasis and its clinical significance. *Altern Ther Health Med* 2009;**15**(3):54–60.
38. Xue C, Shi L, Hui SCN, *et al*. Altered white matter microstructure in the corpus callosum and its cerebral interhemispheric tracts in adolescent idiopathic scoliosis: diffusion tensor imaging analysis. *AJNR Am J Neuroradiol* 2018;**39**(6):1177–84. https://doi.org/10.3174/ajnr.A5634.
39. Shi L, Wang D, Chu WC, *et al*. Volume-based morphometry of brain MR images in adolescent idiopathic scoliosis and healthy control subjects. *AJNR Am J Neuroradiol* 2009;**30**(7):1302–7. https://doi.org/10.3174/ajnr.A1577.
40. Joly O, Rousié D, Jissendi P, *et al*. A new approach to corpus callosum anomalies in idiopathic scoliosis using diffusion tensor magnetic resonance imaging. *Eur Spine J* 2014;**23**(12):2643–9. https://doi.org/10.1007/s00586-014-3435-3.
41. Wang W, Zhu Z, Zhu F, *et al*. Different curve pattern and other radiographical characteristics in male and female patients with adolescent idiopathic scoliosis. *Spine (Phila Pa 1976)* 2012;**37**(18):1586–92. https://doi.org/10.1097/BRS.0b013e3182511d0c.